Diminishing Efficacy of Prone Positioning with Late Application in Evolving Lung Injury

Yi Xin, MS[1], **Kevin Martin, BS**[2], **Caio C.A. Morais, RRT**[3], **Paolo Delvecchio, MS**[2], **Sarah E. Gerard, PhD**[4], **Hooman Hamedani, BS**[1], **Jacob Herrmann, PhD**[5], **Nicholas Abate, BS**[2], **Austin Lenart, BS**[2], **Shiraz Humayun, MD**[2], **Uday Sidhu**[2], **Mihail Petrov, MD**[2], **Kristan Reutlinger, MSN CRNP**[2], **Tal Mandelbaum, MD**[2], **Ian Duncan, PhD**[1], **Nicholas Tustison, PhD**[6], **Stephen Kadlecek, PhD**[1], **Shampa Chatterjee, PhD**[7], **James C. Gee, PhD**[1], **Rahim R. Rizi, PhD**[1], **Lorenzo Berra, MD**[3], **Maurizio Cereda, MD**[1,2]

[1]Department of Radiology, University of Pennsylvania, Philadelphia, PA, USA;

[2]Department of Anesthesiology and Critical Care, University of Pennsylvania, Philadelphia, PA, USA;

[3]Department of Anesthesia, Critical Care and Pain Medicine, Massachusetts General Hospital and Harvard Medical School, Boston, MA, USA;

[4]Department of Radiology, University of Iowa, Iowa City, IA, USA;

[5]Department of Biomedical Engineering, Boston University, Boston, MA, USA;

[6]Department of Radiology and Medical Imaging, University of Virginia, Charlottesville, VA, USA;

[7]Department of Physiology, University of Pennsylvania, Philadelphia, PA, USA

Abstract

Objectives: It is not known how lung injury progression during mechanical ventilation modifies pulmonary responses to prone positioning. We compared the effects of prone positioning on regional lung aeration in late vs. early stages of lung injury.

Design: Prospective, longitudinal imaging study.

Setting: Research imaging facility at The University of Pennsylvania (Philadelphia, PA) and Medical and Surgical Intensive Care Units at Massachusetts General Hospital (Boston, MA).

Subjects: Anesthetized swine and patients with acute respiratory distress syndrome (ARDS)

Corresponding Author: Maurizio Cereda, MD, Department of Anesthesiology and Critical Care, Perelman School of Medicine at the University of Pennsylvania, Dulles 773, 3400 Spruce Street Philadelphia, PA 19104-4283. Tel: (215) 300-1519. maurizio.cereda@pennmedicine.upenn.edu.

Interventions: Lung injury was induced by bronchial hydrochloric acid (HCl, 3.5 ml/kg) in 10 ventilated Yorkshire pigs and worsened by supine non-protective ventilation for 24 hours. Whole-lung computed tomography was performed 2 hours after HCl (Day 1) in both prone and supine positions, and repeated at 24 hours (Day 2). Prone and supine images were registered (superimposed) in pairs to measure the effects of positioning on the aeration of each tissue unit. Two patients with early ARDS were compared to two patients with late ARDS, using electrical impedance tomography to measure the effects of body position on regional lung mechanics.

Measurements and Main Results: Gas exchange and respiratory mechanics worsened over 24 hours, indicating lung injury progression. On Day 1, prone positioning reinflated $18.9 \pm 5.2\%$ of lung mass in the posterior lung regions. On Day 2, position-associated dorsal reinflation was reduced to $7.3 \pm 1.5\%$ ($P<0.05$ vs. Day 1). Prone positioning decreased aeration in the anterior lungs on both days. While prone positioning improved posterior lung compliance in the early ARDS patients, it had no effect in late ARDS subjects.

Conclusions: The effects of prone positioning on lung aeration may depend on the stage of lung injury and duration of prior ventilation; this may limit the clinical efficacy of this treatment if applied late.

INTRODUCTION

While the morphologic and functional characteristics of lungs with acute respiratory distress syndrome (ARDS) change over time (1, 2), this evolution is poorly characterized. Pulmonary stress during mechanical ventilation accelerates ARDS progression (3) and may diminish the efficacy of therapeutic strategies, narrowing the opportunity for successful treatment. Better understanding the evolution of ARDS could therefore help refine both indications and timing of treatment.

Prone ventilation improves gas exchange compared with supine positioning (4) and decreases mortality in severe ARDS (5). Improvements in oxygenation after prone positioning did not predict survival (6), but lower regional tissue stress and more homogeneous gas distribution might explain the outcome effects of this treatment (7, 8). Supporting this hypothesis, serial computed tomography (CT) scans showed that prone ventilation contained the early propagation of experimental lung injury by stabilizing posterior inflation (9). However, only 16 to 33% of patients with severe ARDS receive such treatment (10, 11). Clinicians may view prone positioning as a rescue maneuver (11) and attempt other strategies first, such as higher positive end-expiratory pressure (PEEP) or inhaled vasodilators to increase arterial oxygenation. If injury progression diminishes the lung's ability to improve regional mechanics, delayed initiation could decrease the positive clinical impact of positional therapy. ARDS lungs become resistant to recruitment maneuvers after prolonged ventilation (12), which may explain why the effects of prone

positioning on oxygenation decrease over time (13). However, no experimental studies have prospectively assessed the evolving response of regional lung aeration to positional therapy.

Using paired prone-supine CT images in a large animal model of early lung injury, we found that reaeration and recruitment by the prone position were chiefly localized in posterior lung regions near the diaphragm (14). In the current study, we used a similar imaging approach in ventilated pigs to test the hypothesis that lung injury progression diminishes prone positioning's ability to reaerate the lungs. In addition, we explored the variability in how regional lung mechanics respond to positioning in a small group of patients with late vs. early ARDS.

MATERIALS AND METHODS

Studies were approved by the Animal Care and Use Committee of the University of Pennsylvania and by the Investigational Review Board of the Massachusetts General Hospital (IRB 2019P001995). Figure 1A outlines the animal experiments; detailed methods are described in Supplemental Digital Content 1.

Animal Preparation and Protocol

Ten Yorkshire pigs (30.7 ± 1.1 kg) were anesthetized, intubated, and mechanically ventilated. 3.5 ml/kg of hydrochloric acid (HCl, pH 1.0) was instilled via bronchoscopy into the lobar bronchi. After a two-hour stabilization period, CT scans were obtained (Day 1). All animals were then ventilated supine for 24 hours on volume-controlled ventilation with non-protective settings: PEEP 3 cmH$_2$O and tidal volume (V$_T$) 12 ml/kg. Inspired fraction of oxygen and respiratory rate were set at 0.5 and 25 bpm, respectively, and then adjusted to arterial oxygen saturation (>90%) and PaCO$_2$ (35–45 mmHg). After 24 hours, CT was repeated (Day 2). Hemodynamic and respiratory variables were recorded. Animals were euthanized after Day 2 imaging, lung tissue samples were obtained.

Image Acquisition and Analysis

In the CT scanner, all animals were sequentially placed in both supine and prone positions in random order. After each position change, the animals received a recruitment maneuver. They were then ventilated with each of two settings that were randomly applied for 15 minutes each and followed by CT scans and physiologic measurements: low PEEP (3 cmH$_2$O) non-protective ventilation (V$_T$ 12 ml/kg, rate 25 bpm), and high PEEP (15 cmH$_2$O) ventilation chosen to maximize lung recruitment (Figure 1B). At high PEEP, V$_T$ 6 ml/kg and rate 40 bpm were dialed to avoid barotrauma. Lungs were scanned during 5-second end-expiratory pauses, and images were reconstructed to a resolution of 1×1×1 mm.

To quantitatively analyze aeration changes, we first segmented lung images via validated deep-learning methodology (15) and calculated lung weights (16) and gas volumes (17). We then registered (warped) segmented CT scans obtained in the prone position to the supine images (Figure 1B) using deformable registration to align lung borders and internal features between images, thus placing corresponding voxels on the same reference system (18). This allowed us to measure the effects of positioning and PEEP on the density (aeration) of each voxel. Voxels were then classified as 'recruitment' or 'derecruitment', respectively, if

their density decreased or increased across a threshold of −100 Hounsfield units (HU) with position or PEEP change (14).

Patients

Four patients with ARDS were imaged with electrical impedance tomography (EIT) in both prone and supine positions while volume-control ventilated with V_T 5–6 ml/kg and PEEP 15 cmH$_2$O. At the time of imaging, two of the patients had been ventilated for <7 days ('early ARDS') and two for >7 days ('late ARDS') (19). Images were partitioned into 32 anterior-posterior bins (20). For each bin, tidal ventilation and regional compliance were calculated by impedance changes.

Statistical Analysis

Statistical analysis was performed using RStudio 1.2.5001 (R Foundation for Statistical Computing; Vienna, Austria). Two-tailed paired T-tests with Bonferroni correction were performed for comparisons between time points. A mixed-effect regression model (lme4, R package) (21, 22) was used to study the effects of PEEP, positioning, and their combination (fixed terms) on physiologic and imaging variables. 'Individual subject' was retained as random effect. An experiment-wide P<0.05 was selected as the threshold for statistical significance.

RESULTS

Lung Injury Progression

Acid aspiration worsened gas exchange and respiratory compliance after two hours, followed by further deterioration over the next 24 hours (Figure S1A and Table S1, Supplemental Digital Content 1). Analysis of tissue samples confirmed injury, which was more severe in the middle and lower lobes than in the upper lobe (Figure S1B Supplemental Digital Content 1). Day 1 CT images showed consolidations and ground glass opacities, which became more prominent on Day 2 (Figure 2). Lung weight increased from 764.6±74.7 to 859.9±92.0 grams of tissue (P<0.001) between Days 1 and 2.

Effects of Positioning and PEEP

Respiratory Parameters: On Day 1, prone vs. supine positioning increased PaO$_2$/FiO$_2$ (P<0.001, Cohen's $d = 1.87$) and compliance (P<0.001, Cohen's $d = 1.74$), while high vs. low PEEP decreased both variables (Table S2, Supplemental Digital Content 1). On Day 2, prone positioning slightly worsened PaO$_2$/FiO$_2$ (P=0.003, Cohen's $d = −1.22$) while still increasing compliance (P=0.001, Cohen's d = 1.46); high PEEP had no significant effect on PaO$_2$/FiO$_2$, but worsened compliance similarly to Day 1 (P<0.001, Cohen's $d = −3.19$). PaCO$_2$ was unaffected by positioning on Day 1, but increased in the prone position on Day 2 (P=0.017, Cohen's $d = 0.96$). PaCO$_2$ increased at higher PEEP on both days in both positions, mostly due to the lower V_T. Also see Table S3, Supplemental Digital Content for complete results of the statistical analysis.

Regional Aeration: After segmentation and registration (Figure 2), the effects of PEEP and positioning on regional lung aeration were calculated by subtracting density values

between each voxel of the warped image and the spatially corresponding voxel of the low-PEEP supine scan. The resulting subtraction maps (Figure 3, left panels) show that, on Day 1, proning caused density to decrease (improved aeration) in the posterior-caudal lung (blue) and to increase (worse aeration) in the anterior regions (red). Raising PEEP in the supine animal improved aeration predominantly in the posterior lung. Joint application of high PEEP and prone positioning further enhanced the posterior improvement of aeration. On Day 2, the prone position and high PEEP (alone and in combination) were unable to meaningfully improve posterior and caudal aeration, while their effects on the anterior lung were similar to Day 1.

Lung Recruitment: Voxels of tissue undergoing recruitment or derecruitment were mapped (Figure 3, right panels) and quantified. Most tissue recruited by the prone position was located in the posterior lung regions on Day 1 (Figure 4), but the total amount of recruited tissue diminished from 18.9±5.2% to 7.3±1.5 % of total lung mass (P<0.05) on Day 2. Tissue recruited by high PEEP was also distributed in the posterior territories on Day 1 (Figure 4), but shifted to more anterior regions and decreased from 22.5±5.7% to 15.8±2.9 % of lung mass (P<0.05) on Day 2. Combining prone position and high PEEP enhanced recruitment vs. high PEEP alone on Day 1 (28.3±6.1% vs 22.5±5.7%, P<0.001, Cohen's d = 2.58), while this additional effect was smaller on Day 2 (17.7±4.2% vs 15.8±2.9%, P=0.072, Cohen's d = 0.90). On both days, the prone position was associated with a quota of anterior derecruitment (5.9±3.0% on Day 1, 6.5±2.8% on Day 2) which was attenuated at high PEEP (Figure 4). Also see Tables S4 and S5) in the Online Supplement for recruitment and derecruitment values and complete statistical analysis.

ARDS Patients

Patients were 35 to 69 years old and were ventilated for 6 to 60 days (see text in Supplemental Digital Content 1 for additional details). In patients with "early ARDS" (patients 1 and 2 in Figure 5), prone position increased both global respiratory system compliance and the EIT-measured compliance of the posterior bins, suggesting lung recruitment in the same areas. In "late ARDS" patients (patients 3 and 4 in Figure 5), global compliance was reduced in prone compared to supine position. EIT revealed that regional compliance did not improve in the posterior bins but worsened in the anterior regions.

DISCUSSION

Overall, the results of the animal studies suggest that injury progression in ventilated lungs may lessen prone positioning's ability to improve aeration and recruit posterior lung regions. Furthermore, EIT measurements hint that prone positioning may be unable to improve posterior lung mechanics after prolonged ventilation in clinical ARDS.

Injury Progression and Regional Inflation

Our large animal model mirrored the secondary progression of a primary lung insult. Previous small animal data showed that the evolution of lung injury led to progressive loss of recruitability by PEEP (23). Our study shows that the lungs' ability to respond to prone positioning was similarly altered over time. To quantify these evolving responses, we

performed a detailed analysis of the effects of both prone positioning and PEEP on regional lung inflation. We used our registration method to map lung density shifts with voxel-level resolution (14). In early injury, switching position from supine to prone caused opposing changes in lung aeration in ventral vs. dorsal lung territories: a posterior-caudal region of the lungs was reinflated, while the anterior territory was deflated (Figure 3, left panels), as in previous observations by our group (14) and others (24). These changes were likely due to shifts of the gravitational and non-gravitational forces that deform the lungs (25). However, after 24 hours, the posterior lung region became resistant to these forces. Furthermore, anterior lung deflation was also visible in the prone images on the second day, with the net result of a smaller lung volume than in the supine position (Table S2, Supplemental Digital Content 1).

Previous studies reported that recruitment and derecruitment coexisted when changing body position (26). Using high-resolution analysis, we showed that the net balance between these opposing events shifted during injury progression. In early injury, posterior recruitment was prominent, while derecruitment was smaller and mostly anterior (Figure 4). This favorable balance was likely due to smaller cross section of anterior vs. posterior lung (25). On the second day, derecruitment by prone positioning nearly offset recruitment (Figure 4), suggesting that geometric factors do not guarantee the net beneficial effect of positioning when the posterior lung regions are consolidated. This evolution was paralleled by physiological changes. Recruitment in the posterior-caudal region, which was likely well perfused (27), explains the effect of positioning on oxygenation on the first day, while neither recruitment nor PaO2 improved in late injury. In absence of perfusion data, we cannot definitively determine whether the higher $PaCO_2$ observed in the prone vs. supine position on Day 2 was primarily related to regional hypoventilation or blood flow redistribution. This negative response could be a marker of deteriorating lung conditions. In contrast, improved $PaCO_2$ after prone positioning was associated with higher lung recruitability (28) and survival (29) in ARDS patients. Recruitment can also explain increased compliance with prone positioning on Day 1, although this mechanism does not completely account for the higher compliance also observed on Day 2, when recruitment by prone positioning was minimal. It is possible that restrained anterior inflation improved chest wall mechanics enough to offset the lack of net recruitment in the prone position (30).

Image registration enabled us to observe that, when applied separately in late injury, PEEP and prone positioning recruited non-overlapping regions of lung (Figures 3, 4): tissue recruited at high PEEP was more anterior in late vs. early injury since the posterior lung had become harder to reinflate. Despite recruitment, high PEEP worsened compliance on both days of the study, which was probably due to maximized inflation in the anterior region. This state was likely associated with anterior lung hypoperfusion (31), contributing to lower oxygenation at higher PEEP.

Biologic Mechanisms

Fibroproliferative responses occur early in both human (32) and experimental (33) lung injury, and are likely involved in the loss of positional response in our patients (19). However, fibrosis is unlikely to have measurable physiologic and radiologic consequences in

the timeframe of our animal studies. Edema could explain the loss of posterior recruitability observed in our study, as suggested by the increased tissue weight, but it is also likely that supine ventilation provoked progressive induration of lung tissue, as described in an acid aspiration model (23). This evolution is probably mediated by protein accumulation in the airspaces and resulting surfactant deterioration (23), which increases the tendency to unrecoverable derecruitment (34).

Clinical Implications

Cornejo *et al.* showed smaller effects of positioning in ARDS patients with poorly recruitable lungs (35). Although other factors such as origin of injury (16) are likely involved, our experimental results suggest that the stage of disease could contribute to variability of treatment responses.

The most successful clinical trial on prone positioning (5) showed a strong outcome benefit when treatment was applied within 72 hours of onset. Nevertheless, initiation of positional therapy is often delayed or replaced by other treatments with less established clinical efficacy (36). Among other factors, incomplete knowledge of the injury-containing effects of positional therapy hinders its implementation (37). Our experimental results provide a physiological rationale to avoid delaying treatment, corroborating reports of decreased lung recruitability in late vs. early ARDS (12). Furthermore, we suggest posterior lung recruitability as a possible early marker of the potential clinical success of prone positioning. Animal studies by our group (9) and others show that improved inflation in the posterior lung may help contain early injury progression (38). Future human studies could confirm the temporal evolution of such positional responses and reveal correlations with outcomes.

While our exploratory EIT measurements were performed in a small number of patients with scattered timing from ARDS onset, they nevertheless illustrate how this instrument, although limited by low spatial resolution, can visualize the variable effects of prone positioning in human ARDS. Regional responses may be particularly relevant in obese patients, who suffer from posterior lung collapse and benefit disproportionately from positional therapy (39), or in COVID-19 patients, in whom prone positioning is used extensively (40) but in whom lung recruitability might be low (41). Patients with reactivation of lung injury during protracted ventilation can also benefit from topographic assessment of positional inflation changes.

Limitations

The acid aspiration model has important limitations: it does not comprehend complex injury mechanisms observed in clinical ARDS, e.g. from sepsis, and lungs are less recruitable than in other models. Nevertheless, we chose acid aspiration because it recapitulated the evolution of a primary insult to the lungs in previous studies (42).

We ventilated animals for 24 hours with non-protective settings to accelerate injury progression, which limits the clinical extrapolation of our results—although lung-protective ventilation did not prevent worsening of lung strain distribution in supine sheep (8). During animal imaging, we chose a large gradient between tested PEEP levels because response to this PEEP range is a good predictor of maximum recruitability (16). However, a smaller PEEP difference could have produced better functional results. We chose different tidal

volumes between tested PEEP levels to limit lung overdistension and barotrauma during high PEEP while also avoiding lethal hypoxemia during low PEEP. Finally, ventilator settings and body positions were applied in-scanner for relatively short intervals: longer wait times (hours) would likely have enhanced the gas exchange effects of prone positioning (43, 44) but would have been impractical. However, serial CT scans confirmed that inflation distribution was not substantially altered while waiting for up to one hour in the prone position (Figure S2, Online Supplement).

While faulty registration can induce errors in voxel-level measurements of inflation shifts due to higher PEEP and positional changes, we have previously provided reassuring data showing that major airway structures (9, 14), outer lung borders (45), and inflation distributions (9, 14, 42) are reasonably preserved after warping. Finally, we cannot discriminate between the effects of chest wall and lung mechanics on regional inflation, respectively, in the absence of esophageal manometry.

CONCLUSIONS

In conclusion, the results of this study in an animal model support the hypothesis that evolving lung injury is characterized by a time-dependent loss of aeration response to prone positioning in the posterior lung. This deterioration probably contributes to variability in responses to positional therapy, and might undermine the clinical outcome benefits of this treatment.

Supplementary Material

Refer to Web version on PubMed Central for supplementary material.

ACKNOWLEDGMENTS

REFERENCES

1. Gattinoni L, Bombino M, Pelosi P, et al.: Lung structure and function in different stages of severe adult respiratory distress syndrome. JAMA1994; 271:1772–1779 [PubMed: 8196122]

2. Matamis D, Lemaire F, Harf A, et al.: Total respiratory pressure-volume curves in the adult respiratory distress syndrome. Chest1984; 86:58–66 [PubMed: 6734293]

3. Network TARDS: Ventilation with Lower Tidal Volumes as Compared with Traditional Tidal Volumes for Acute Lung Injury and the Acute Respiratory Distress Syndrome. New England Journal of Medicine2000; 342:1301–1308

4. Richter T, Bellani G, Harris RS, et al.: Effect of Prone Position on Regional Shunt, Aeration, and Perfusion in Experimental Acute Lung Injury. Am J Respir Crit Care Med2005; 172:480–487 [PubMed: 15901611]

5. Guerin C, Reignier J, Richard JC, et al.: Prone positioning in severe acute respiratory distress syndrome. The New England journal of medicine2013; 368:2159–2168 [PubMed: 23688302]

6. Albert RK, Keniston A, Baboi L, et al.: Prone position–induced improvement in gas exchange does not predict improved survival in the acute respiratory distress syndrome. American journal of respiratory and critical care medicine2014; 189:494–496 [PubMed: 24528322]

7. Gattinoni L, Pelosi P, Vitale G, et al.: Body position changes redistribute lung computed-tomographic density in patients with acute respiratory failure. Anesthesiology1991; 74:15–23 [PubMed: 1986640]

8. Motta-Ribeiro GC, Hashimoto S, Winkler T, et al.: Deterioration of Regional Lung Strain and Inflammation during Early Lung Injury. Am J Respir Crit Care Med2018; 198:891–902 [PubMed: 29787304]

9. Xin Y, Cereda M, Hamedani H, et al.: Unstable Inflation Causing Injury. Insight from Prone Position and Paired Computed Tomography Scans. American Journal of Respiratory and Critical Care Medicine2018; 198:197–207 [PubMed: 29420904]

10. Bellani G, Laffey JG, Pham T, et al.: Epidemiology, Patterns of Care, and Mortality for Patients With Acute Respiratory Distress Syndrome in Intensive Care Units in 50 Countries. Jama2016; 315:788–800 [PubMed: 26903337]

11. Guérin C, Beuret P, Constantin JM, et al.: A prospective international observational prevalence study on prone positioning of ARDS patients: the APRONET (ARDS Prone Position Network) study. Intensive Care Medicine2018; 44:22–37 [PubMed: 29218379]

12. Grasso S, Mascia L, Del Turco M, et al.: Effects of recruiting maneuvers in patients with acute respiratory distress syndrome ventilated with protective ventilatory strategy. Anesthesiology2002; 96:795–802 [PubMed: 11964585]

13. Gattinoni L, Tognoni G, Pesenti A, et al.: Effect of prone positioning on the survival of patients with acute respiratory failure. New England Journal of Medicine2001; 345:568–573

14. Xin Y, Cereda M, Hamedani H, et al.: Positional Therapy and Regional Pulmonary Ventilation: High-resolution Alignment of Prone and Supine Computed Tomography Images in a Large Animal Model. Anesthesiology2020; 133:1093–1105 [PubMed: 32773690]

15. Gerard SE, Herrmann J, Kaczka DW, et al.: Multi-resolution convolutional neural networks for fully automated segmentation of acutely injured lungs in multiple species. Medical Image Analysis2020; 60:101592 [PubMed: 31760194]

16. Gattinoni L, Caironi P, Cressoni M, et al.: Lung Recruitment in Patients with the Acute Respiratory Distress Syndrome. New England Journal of Medicine2006; 354:1775–1786

17. Patroniti N, Bellani G, Manfio A, et al.: Lung volume in mechanically ventilated patients: measurement by simplified helium dilution compared to quantitative CT scan. Intensive Care Medicine2004; 30:282–289 [PubMed: 14714108]

18. Tustison NJ, Avants BB: Explicit B-spline regularization in diffeomorphic image registration [Internet]. Front Neuroinform2013; 7Available from: http://www.ncbi.nlm.nih.gov/pmc/articles/PMC3870320/

19. Fukuda Y, Ishizaki M, Masuda Y, et al.: The role of intraalveolar fibrosis in the process of pulmonary structural remodeling in patients with diffuse alveolar damage. Am J Pathol1987; 126:171–182 [PubMed: 3812636]

20. Costa EL, Lima RG, Amato MB: Electrical impedance tomography. Current Opinion in Critical Care2009; 15:18–24 [PubMed: 19186406]

21. Introduction to Mixed Modelling: Beyond Regression and Analysis of Variance | Wiley [Internet]. Wiley.com [cited 2020 Oct 13] Available from: https://www.wiley.com/en-us/Introduction+to+Mixed+Modelling%3A+Beyond+Regression+and+Analysis+of+Variance-p-9780470035962

22. Bates D, Mächler M, Bolker B, et al.: Fitting Linear Mixed-Effects Models Using lme4. Journal of Statistical Software2015; 67:1–48

23. Allen GB, Leclair T, Cloutier M, et al.: The response to recruitment worsens with progression of lung injury and fibrin accumulation in a mouse model of acid aspiration. American Journal of Physiology-Lung Cellular and Molecular Physiology2007; 292:L1580–L1589 [PubMed: 17351059]

24. Albert RK, Leasa D, Sanderson M, et al.: The prone position improves arterial oxygenation and reduces shunt in oleic-acid-induced acute lung injury. Am Rev Respir Dis1987; 135:628–633 [PubMed: 3030168]

25. Hubmayr RD, Walters BJ, Chevalier PA, et al.: Topographical distribution of regional lung volume in anesthetized dogs. J Appl Physiol Respir Environ Exerc Physiol1983; 54:1048–1056 [PubMed: 6853280]

26. Richard JC, Bregeon F, Costes N, et al.: Effects of prone position and positive end-expiratory pressure on lung perfusion and ventilation. Crit Care Med2008; 36:2373–2380 [PubMed: 18596639]

27. Altemeier WA, McKinney S, Krueger M, et al.: Effect of posture on regional gas exchange in pigs. J Appl Physiol2004; 97:2104–2111 [PubMed: 15298981]

28. Protti A, Chiumello D, Cressoni M, et al.: Relationship between gas exchange response to prone position and lung recruitability during acute respiratory failure. Intensive Care Med2009; 35:1011–1017 [PubMed: 19189081]

29. Gattinoni L, Vagginelli F, Carlesso E, et al.: Decrease in PaCO2 with prone position is predictive of improved outcome in acute respiratory distress syndrome. Crit Care Med2003; 31:2727–2733 [PubMed: 14668608]

30. Galiatsou E, Kostanti E, Svarna E, et al.: Prone Position Augments Recruitment and Prevents Alveolar Overinflation in Acute Lung Injury. American Journal of Respiratory and Critical Care Medicine2006; 174:187–197 [PubMed: 16645177]

31. Musch G, Harris RS, Vidal Melo MF, et al.: Mechanism by Which a Sustained Inflation Can Worsen Oxygenation in Acute Lung Injury. Anesthesiology2004; 100:323–330 [PubMed: 14739807]

32. Chesnutt AN, Matthay MA, Tibayan FA, et al.: Early detection of type III procollagen peptide in acute lung injury. Pathogenetic and prognostic significance. American Journal of Respiratory and Critical Care Medicine1997; 156:840–845 [PubMed: 9310002]

33. Curley GF, Contreras M, Higgins B, et al.: Evolution of the Inflammatory and Fibroproliferative Responses during Resolution and Repair after Ventilator-induced Lung Injury in the Rat. Anesthesiology2011; 115:1022–1032 [PubMed: 21952251]

34. Gaver III DP, Nieman GF, Gatto LA, et al.: The POOR Get POORer: A Hypothesis for the Pathogenesis of Ventilator-Induced Lung Injury [Internet]. Am J Respir Crit Care Med2020; [cited2020 Oct 6] Available from: https://www.atsjournals.org/doi/abs/10.1164/rccm.202002-0453CP

35. Cornejo RA, Díaz JC, Tobar EA, et al.: Effects of Prone Positioning on Lung Protection in Patients with Acute Respiratory Distress Syndrome. Am J Respir Crit Care Med2013; 188:440–448 [PubMed: 23348974]

36. Li X, Scales DC, Kavanagh BP: Unproven and Expensive before Proven and Cheap: Extracorporeal Membrane Oxygenation versus Prone Position in Acute Respiratory Distress Syndrome. Am J Respir Crit Care Med2018; 197:991–993 [PubMed: 29313706]

37. Klaiman T, Silvestri JA, Srinivasan T, et al.: Improving Prone Positioning for Severe Acute Respiratory Distress Syndrome during the COVID-19 Pandemic. An Implementation-Mapping Approach. Ann Am Thorac Soc2021; 18:300–307 [PubMed: 33522870]

38. Broccard A, Shapiro RS, Schmitz LL, et al.: Prone positioning attenuates and redistributes ventilator-induced lung injury in dogs. Critical care medicine2000; 28:295–303 [PubMed: 10708156]

39. De Jong A, Molinari N, Sebbane M, et al.: Feasibility and effectiveness of prone position in morbidly obese patients with ARDS: a case-control clinical study. Chest2013; 143:1554–1561 [PubMed: 23450309]

40. Grasselli G, Pesenti A, Cecconi M: Critical Care Utilization for the COVID-19 Outbreak in Lombardy, Italy: Early Experience and Forecast During an Emergency Response. JAMA2020; 323:1545 [PubMed: 32167538]

41. Ball L, Robba C, Maiello L, et al.: Computed tomography assessment of PEEP-induced alveolar recruitment in patients with severe COVID-19 pneumonia. Critical Care2021; 25:81 [PubMed: 33627160]

42. Cereda M, Xin Y, Hamedani H, et al.: Tidal changes on CT and progression of ARDS. Thorax2017; thoraxjnl-2016–209833 Volume 72, Issue 11

43. Miyamoto K, Kawazoe Y, Yasuda M, et al.: Oxygenation improves during the first 8 h of extended-duration prone positioning in patients with respiratory failure: a retrospective study. j intensive care2014; 2:52 [PubMed: 25705410]

44. Jochmans S, Mazerand S, Chelly J, et al.: Duration of prone position sessions: a prospective cohort study. Ann Intensive Care2020; 10:66 [PubMed: 32449068]

45. Xin Y, Song G, Cereda M, et al.: Semiautomatic segmentation of longitudinal computed tomography images in a rat model of lung injury by surfactant depletion. Journal of Applied Physiology2015; 118:377–385 [PubMed: 25640150]
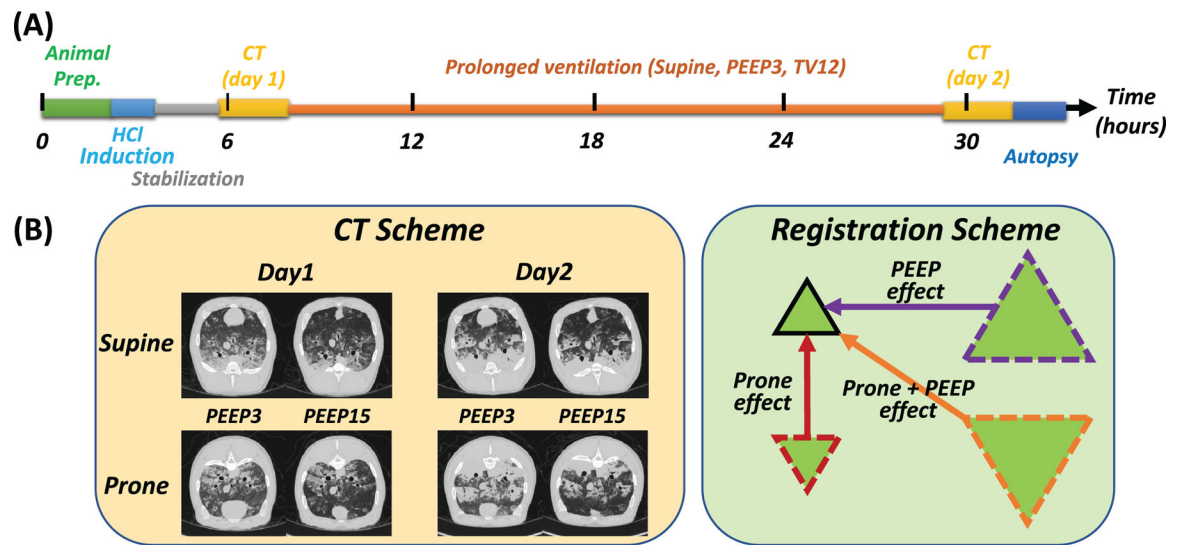
Figure 1.

A) Experimental timeline in supine pigs ventilated with non-protective settings after hydrochloric acid (HCl) instillation in the bronchi. After animal preparation and HCl administration, pigs were stabilized for two hours, followed by early (Day 1) computed tomography (CT) scans. All pigs were then ventilated with tidal volume (V_T) 12 ml/kg and positive end-expiratory pressure (PEEP) 3 cmH$_2$O. After 24 hours, CT scans were repeated (Day 2), followed by euthanasia and tissue retrieval. B) On both days, CT scans (left panel inserts) were obtained during end-expiratory pauses following 15-minute-long periods of ventilation in prone or supine position with low (3 cmH$_2$O) or high (15 cmH$_2$O) PEEP, applied in random order. For image processing (right panel), CT scans in the prone position at low and high PEEP, and in the supine (at high PEEP) positions were registered to (superimposed on) supine-low PEEP scans.
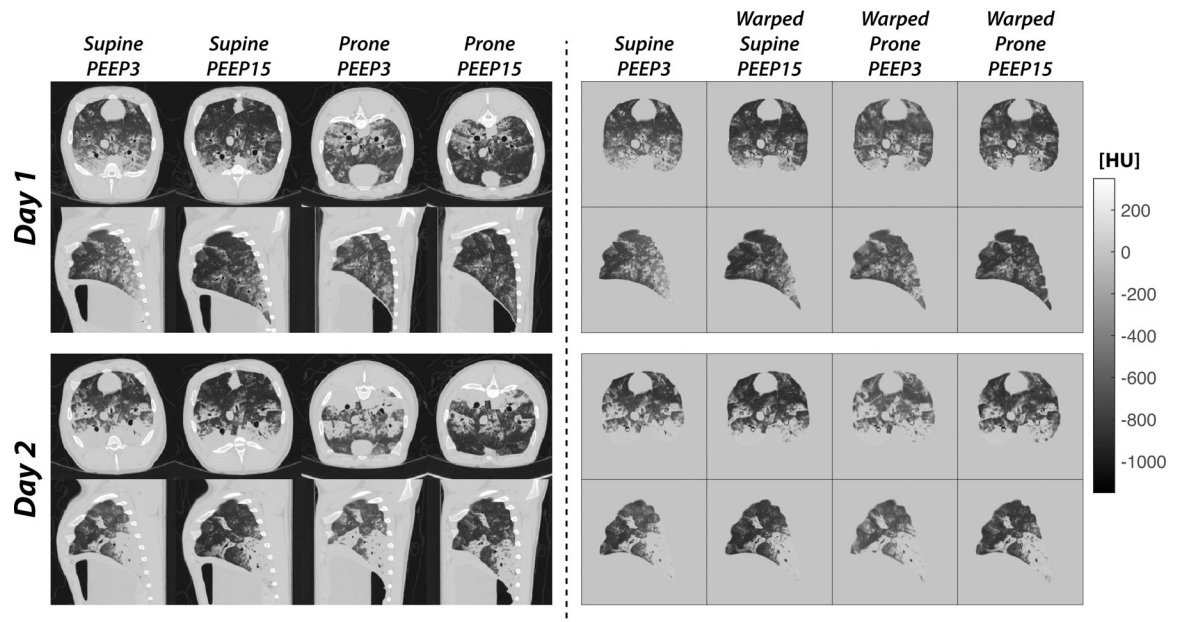
Figure 2.
Representative axial and coronal images obtained in early acid aspiration injury (Day 1) and after 24 hours of ventilation with non-protective settings (Day 2). The left panels show the unprocessed images, which were obtained during expiratory pauses after ventilation in both supine and prone positions at two levels of PEEP. Day 2 images show the radiological progression of lung injury, with expansion of high-attenuation areas. The right panels show the same images after segmentation and registration (warping). All images were registered to the supine-low PEEP scans obtained on the same day, which were used as a reference to create high-resolution maps of the changes in aeration resulting from the tested treatments. In this figure, the warped prone images are inverted to facilitate anatomic comparisons.
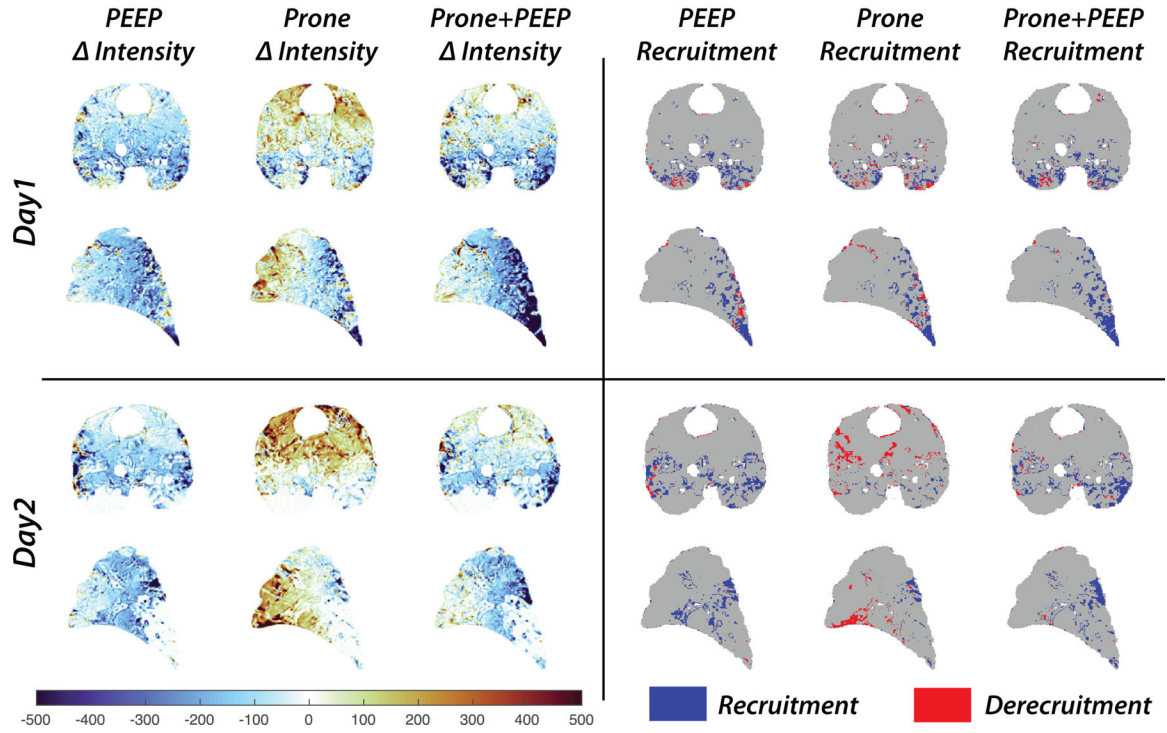
Figure 3.
Subtraction maps display voxel-by-voxel density changes (left panels) and lung recruitment-derecruitment (right panels) on Day 1 (upper panels) and Day 2 (lower panels) of the experiment. The density changes were calculated by subtracting the CT densities of the warped images from those of the supine-low PEEP images, which were used as a reference to calculate the effects on the gas content of each voxel of high PEEP alone, prone position alone, and their joint application. Recruitment and derecruitment were mapped by identifying voxels where the CT density changes due to PEEP or positioning crossed a threshold (−100 Hounsfield Units) indicating near complete loss of aeration. Recruited voxels are shown in blue; derecruitment is shown in red.
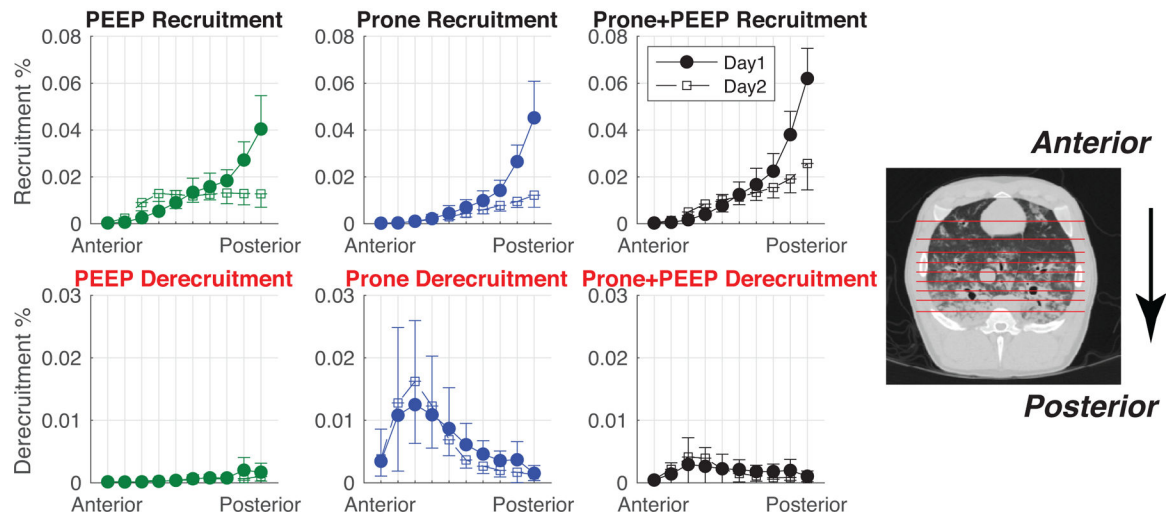
Figure 4.

The regional distributions of recruitment and derecruitment were analyzed by partitioning the lung into 10 segments with equal numbers of voxels along the Anterior-Posterior axis, as exemplified in the images on the right. Each value (mean±SD) represents the amount of recruited or derecruited tissue (as a % fraction of the total lung volume) contained in each bin. Day 1 (closed circles) and Day 2 (open squares) are shown in each plot.
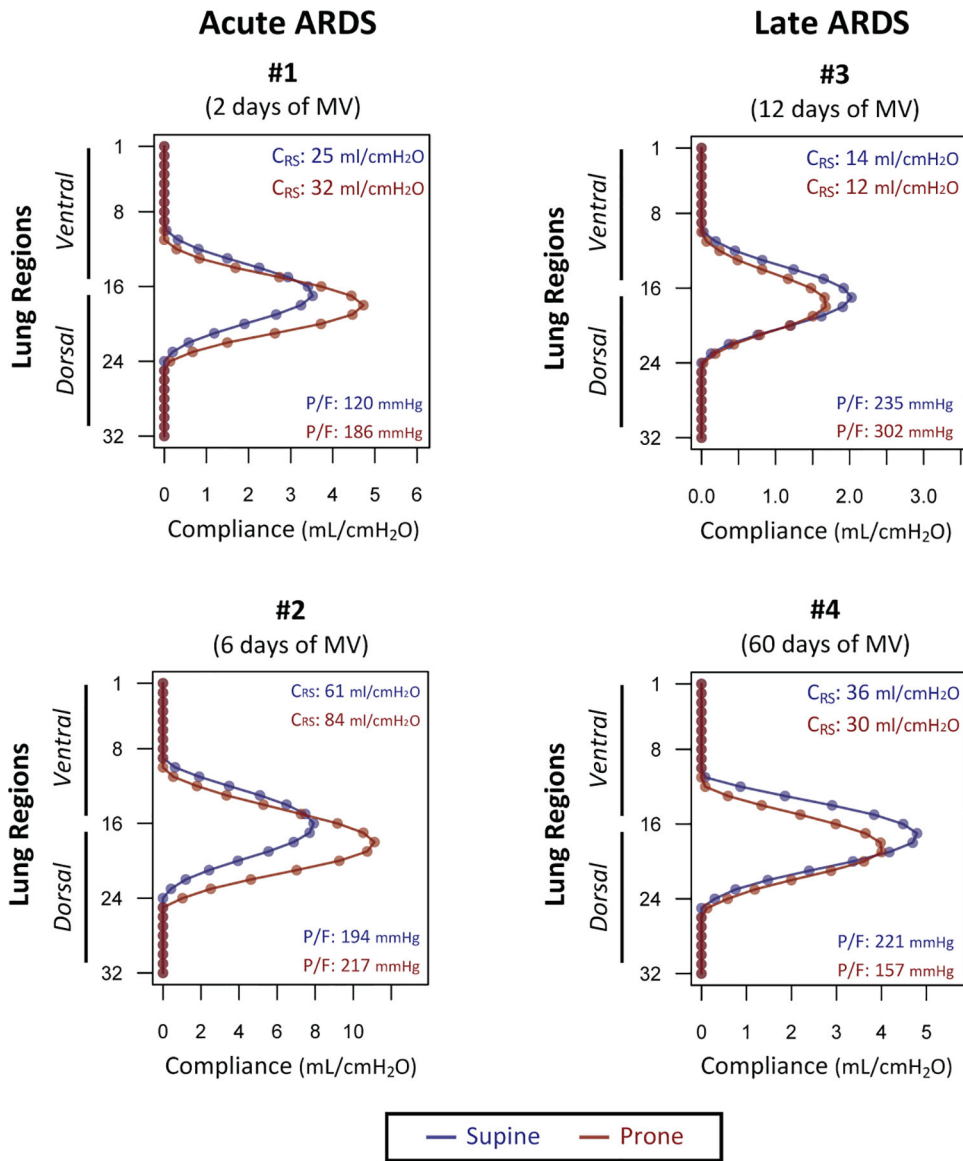
Figure 5.
Changes in regional compliance measured by electrical impedance tomography (EIT) in 32 horizontal bins (region 1: most anterior, region 32: most posterior) in patients with early and late ARDS imaged in supine (blue) and prone (in red) positions. Global respiratory system compliance (CRS) and PaO_2/FiO_2 ratio (P/F) were added to each graph for each position. Please note that regional ventilation and compliance are measurable mostly in the central bins (e.g. 8–24), as the more peripheral bin values reflect extrapulmonary tissue impedance.